SIAM J. SCI. COMPUT.
Vol. 35, No. 4, pp. B890–B911

ADAPTIVE DISCONTINUOUS GALERKIN METHOD FOR RESPONSE-EXCITATION PDF EQUATIONS*

H. CHO†, D. VENTURI†, AND G. E. KARNIADAKIS†

Abstract. Evolution equations of the joint response-excitation probability density function (REPDF) generalize the existing PDF evolution equations and enable us to compute the PDF of the solution of stochastic systems driven by colored random noise. This paper aims at developing an efficient numerical method for this evolution equation of REPDF by considering the response and excitation spaces separately. For the response space, a nonconforming adaptive discontinuous Galerkin method is used to resolve both local and discontinuous dynamics while a probabilistic collocation method is used for the excitation space. We propose two fundamentally different adaptive schemes for the response space using either the local variance combined with the boundary flux difference or using particle trajectories. The effectiveness of the proposed new algorithm is demonstrated in two prototype applications dealing with randomly forced nonlinear oscillators. We first study the stochastic pendulum problem and compare the resulting PDF against the one obtained from Monte Carlo simulation. Subsequently, we study the Duffing oscillator for two different types of stochastic forcing and random initial conditions. We observe both oscillatory and chaotic dynamics and compare the results against the solution of the effective Fokker–Planck equation. The framework we develop here is general and can be readily extended to stochastic PDEs subject to random boundary conditions, random initial conditions, or random forcing terms.

Key words. colored random noise, high-dimensional stochastic dynamical systems, uncertainty quantification

AMS subject classifications. 60H35, 34F05, 65M70

DOI. 10.1137/12088896X

1. Introduction.

Investigations on probabilistic solutions to system of stochastic differential equations have recently received a considerable amount of interest, for many important problems in science and engineering are modeled as such systems [1, 29, 36, 40]. In addition, novel types of dynamics have been found in the presence of this randomness, generally referred to as the noise-induced effects, such as stochastic bifurcations [39, 67] and stochastic resonances [69]. Gaussian white noise has long been employed in many theoretical studies because of its mathematical simplicity. However, various theoretical and numerical attempts have been made to obtain more realistic models for physical and biological systems by considering colored noise [9,20,23,31,37,65]. Therefore, it has become clear that we need to obtain a generalized approach that can model and analyze a broader type of noise in stochastic systems.

The statistics of stochastic dynamical systems can be fully analyzed by the use of a probability density function (PDF) of the solution. Evolution equations for the response PDF have been developed for various systems, such as the Liouville equation or the Fokker–Planck equation [47]. Solving the PDF evolution equation has the advantage of capturing the entire stochastic structure, while many well-known approaches for uncertainty quantification aim at computing the first few statistical moments associated with the solution, e.g., the generalized polynomial chaos [21, 66],

*Submitted to the journal's Computational Methods in Science and Engineering section August 23, 2012; accepted for publication (in revised form) June 7, 2013; published electronically August 13, 2013. This work was supported by OSD-MURI grant FA9550-09-1-0613, by DOE and by NSF/DMS.
http://www.siam.org/journals/sisc/35-4/88896.html
†Division of Applied Mathematics, Brown University, Providence, RI 02912 (heyrim_cho@brown.edu, daniele_venturi@brown.edu, george_karniadakis@brown.edu).

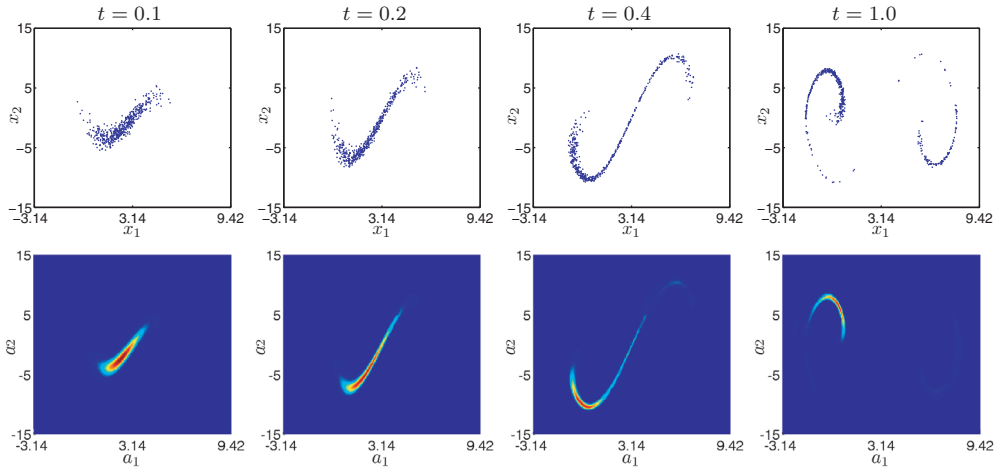

FIG. 1.1. *Comparison between the sample phase space (first row) and the joint PDF of the position and the momentum of a randomly forced nonlinear pendulum (second row) (for a detailed description of this problem see section* 4.1*). The PDF solution is obtained by using the proposed adaptive discontinuous Galerkin method. It is seen that the position of the sample particles are in very good agreement with the computed PDF at different times.*

multielement generalized polynomial chaos [62,64], multielement and sparse grid adaptive probabilistic collocation [18,44], stochastic biorthogonal expansions [52,55,56,61], and generalized spectral decompositions [35, 42, 43]. PDF based methods usually cost more to compute than moment based methods, since they carry more information. However, when the system is complex, as in Figure 1.1 where the PDF of the pendulum splits into two different positions, the dynamics in the stochastic domain cannot be captured only by the first few moments, but can only be understood by observing the entire PDF; see also [37]. In the context of uncertainty quantification (UQ), PDF methods allow us to accurately capture rare events by the tails of the probabilistic distributions. Yet the application of existing PDF equations is limited to certain types of systems. For example, the Liouville equation can be used when the randomness lies only in the initial condition whereas the Fokker–Planck equation can be applied to systems driven by white noise. In particular, the Fokker–Planck equation has been extended to more general random forcing, e.g., with finite correlation time [53]. However, it always involves certain approximations to make it computable, such as the limiting case of small correlation length [9, 31].

The evolution equation of the joint response-excitation probability density function (REPDF) has been proposed recently, generalizing the existing PDF evolution equations [51, 60]. By considering the equation on the expanded joint space of the solution and excitation, exact evolution equations can be obtained for any stochastic dynamical system with random initial conditions, random coefficients, or random forcing including colored noise. The evolution equation of REPDF for a dynamical system has been derived long time ago by Dostupov and Pugachev [15], and more recently by Li and Chen [36] by using conservation of probability arguments. However, the REPDF equation can be obtained even for partial differential equations, such as scalar PDEs of first order [59] or more general PDEs [38, 58]. The advantage of the REPDF equation is that it is linear, deterministic, and of first order. The main drawback is the increased dimensionality, since the REPDF equation has to be solved on a domain involving all the random excitation dimensions. In addition to the dimensionality issue, the PDF of the system can be compactly supported and very steep (see Figure 1.1).

The purpose of this paper is to develop an efficient numerical method to compute the solution of the joint REPDF equation corresponding to an arbitrary nonlinear stochastic dynamical system. This allows us to address the question of whether the joint REPDF approach can provide an effective computational tool to simulate the effects of *colored random noise* in physical systems. The numerical challenges associated with this task are twofold. First the dimensionality, which may be eventually handled by using closures or techniques for high-dimensional systems; and second, the solution which may be *discontinuous* and *compactly supported* over disjoint domains (see Figure 1.1). This obviously requires the development of appropriate numerical techniques, such as the adaptive discontinuous Galerkin method [11] considered in this paper. In order to improve the computational efficiency, we have also developed *nonconforming* adaptive strategies based on two different adaptive criteria: (1) a combination of local variance and boundary flux difference, and (2) a concentration of sample points in phase space.

This paper is organized as follows. In section 2 we present the joint REPDF equations that will be discretized numerically by using the techniques discussed in section 3. The effectiveness of the proposed algorithms is demonstrated in the numerical applications presented in section 4. Finally, the main findings and their implications are summarized in section 5.

2. Kinetic equation for the joint REPDF. Let us consider the following nonlinear stochastic dynamical system

$$\frac{dx(t;\omega)}{dt} = G(x(t;\omega),\xi(\omega),t), \qquad x(t_0;\omega) = x_0(\omega), \tag{2.1}$$

where $x(t;\omega) \in \mathbb{R}^n$ is a multidimensional stochastic process, while $\xi(\omega) \in \mathbb{R}^m$ and $x_0(\omega) \in \mathbb{R}^n$ are random variables with known joint probability function. The stochastic system (2.1) can be high dimensional as it can arise, for instance, from a discretization of a stochastic PDE (SPDE) subject to random boundary conditions, random initial conditions, or random forcing terms.[1] The existence and the uniqueness of the solution to (2.1) for each realization of $\xi(\omega)$ and $x_0(\omega)$ allows us to consider the stochastic flow $x(t;\omega)$ as a deterministic function of $\xi(\omega)$ and $x_0(\omega)$, i.e., $x(t;\omega) = x(t;\xi(\omega),\, x_0(\omega))$.

Under this hypothesis, by using the response-excitation theory [15, 36, 60] it is straightforward to obtain an exact closed equation for the joint REPDF of the random vectors $x(t;\omega)$ and $\xi(\omega)$, namely,

$$p^{(a,b)}_{x(t)\xi} \stackrel{\text{def}}{=} \langle \delta(a - x(t;\omega))\, \delta(b - \xi(\omega)) \rangle\,, \qquad t \geq t_0\,, \quad a \in \mathbb{R}^n\,, \quad b \in \mathbb{R}^m\,, \tag{2.2}$$

where the average operator $\langle\cdot\rangle$ is with respect to the joint PDF of the random input variables $\xi(\omega)$ and $x_0(\omega)$, while δ denotes a multidimensional Dirac delta function, i.e.,

$$\delta(a - x(t;\omega)) \stackrel{\text{def}}{=} \prod_{k=1}^{n} \delta(a_k - x_k(t;\omega))\,, \qquad \delta(b - \xi(\omega)) \stackrel{\text{def}}{=} \prod_{k=1}^{m} \delta(b_k - \xi_k(\omega))\,.$$

The evolution equation for the joint REPDF (2.2) can be derived by differentiating

[1] In this case, the phase space variables $x_j(t;\omega)$ could be the Galerkin or the collocation coefficients of an expansion of the solution relatively to suitable spatial basis function $\phi_j(x)$, i.e., $u(x,t;\omega) = \sum_{j=1}^{n} x_j(t;\omega)\phi_j(x)$.

the functional integral representation (2.2) with respect to t. By using well-known identities involving the Dirac delta function [32, 33, 60], we obtain

$$\frac{\partial p^{(a,b)}_{x(t)\xi}}{\partial t} = \mathcal{L}(t) p^{(a,b)}_{x(t)\xi}\,, \tag{2.3}$$

where

$$\mathcal{L}(t) \stackrel{\text{def}}{=} -\sum_{i=1}^{n} \frac{\partial G_i(a,b,t)}{\partial a_i} - \sum_{i=1}^{n} G_i(a,b,t)\frac{\partial}{\partial a_i}$$

is a *first-order* (time-dependent) linear partial differential operator in n variables $(a_1, \ldots, a_n)$ and m parameters $(b_1, \ldots, b_m)$. Time dependence can arise, e.g., due to time-dependent random boundary conditions in SPDEs or time-dependent random forcing terms in SODEs.

The REPDF equation (2.3) is supplemented with appropriate boundary conditions and with the initial condition $p^{(a,b)}_{x(t_0)\xi}$, expressing the joint PDF of $x_0(t_0;\omega)$ and $\xi(\omega)$. Kinetic equations of type (2.3) were determined long ago by Dostupov and Pugachev in [15]. More recently, Li and Chen [36] introduced a similar theory in the context of stochastic dynamics of structures (see [36, Chaps. 7–8] and [7]) by using conservation of probability arguments.

We notice that the REPDF equation (2.3) is analogous to the Liouville equation of classical statistical mechanics, as it governs the evolution of the joint PDF of the phase space. This analogy can be exploited even further by noting that the ODE system (2.1) can be rewritten as a larger system subject only to a random initial condition. To this end, it is sufficient to define a new set of phase variables $y(t;\omega)$ evolving according to

$$\frac{dy(t;\omega)}{dt} = 0\,, \qquad y(t_0;\omega) = \xi(\omega)\,, \qquad y(t;\omega) \in \mathbb{R}^m\,, \tag{2.4}$$

and replace the vector $\xi(\omega)$ in (2.1) with $y(t;\omega)$. This yields

$$\frac{dx(t;\omega)}{dt} = G(x(t;\omega), y(t;\omega), t)\,, \qquad x(t_0;\omega) = x_0(\omega)\,. \tag{2.5}$$

The system (2.4)–(2.5) is equivalent to (2.1), but now the random variables $\xi(\omega)$ appear as an initial condition for $y(t;\omega)$. In this form the Liouville theory applies, leading us to the joint REPDF equation (2.3).

Time integration schemes for (2.3) relying directly on formal representations, such as Magnus expansions [4], usually require the computation of exponential operators involving $\mathcal{L}(t)$. As a result of discretization of the phase space, $\mathcal{L}(t)$ typically becomes a very large matrix and, as a consequence, the exponentiation operation is exceedingly costly [49, 54].

3. Numerical method. It is convenient to group the independent variables appearing in the solution to the joint REPDF equation (2.3) into two main classes, i.e., those belonging to the *response space* and those belonging to the *excitation space*. The response space is a subset of $\mathbb{R}^n$ that includes the phase variables a. These variables are differentiated in the PDF equation (2.3). On the other hand, the excitation space is a subset of $\mathbb{R}^m$ that includes the variables b, which appear simply as parameters in (2.3). Different numerical techniques are described hereafter for the discretization of the response and the excitation spaces.

3.1. Response space. The response space can be discretized by using an adaptive discontinuous Galerkin (DG) method [11, 12], possibly combined with functional ANOVA techniques [6]. As is well known, the DG method has many good features of both finite volume and finite element methods, such as flexibility and *hp*-adaptivity.

3.1.1. Discontinuous Galerkin formulation. In order to illustrate the application of the DG method to the joint REPDF equation (2.3), let us rewrite it in the form of the hyperbolic conservation law, i.e.,

$$\frac{\partial p^{(a,b)}_{x(t)\xi}}{\partial t} = -\nabla_a \cdot \left(G(a,b,t) p^{(a,b)}_{x(t)\xi} \right) , \tag{3.1}$$

where ∇_a denotes the multidimensional gradient operator with respect to the variables $a \in \mathbb{R}^n$. It is convenient at this point to define the multidimensional flux

$$F[p] \stackrel{\text{def}}{=} G(a,b,t) p^{(a,b)}_{x(t)\xi} , \tag{3.2}$$

where we have emphasized the functional dependence on $p^{(a,b)}_{x(t)\xi}$ by using the notation $F[p]$. Next, we consider a finite element discretization of the response space, i.e., the phase space described by the variables $a \in \mathbb{R}^n$. Specifically, we select a bounded computational domain $\Omega \subseteq \mathbb{R}^n$, which is large enough to include the support of the joint REPDF $p^{(a,b)}_{x(t)\xi}$. This allows us to set a zero homogeneous boundary condition at the boundary of Ω. Let Ω_h be a triangulation of Ω, consisting of elements K_i $(i = 1, \ldots, N_{el})$, i.e.,

$$\Omega = \bigcup_{i=1}^{N_{el}} K_i , \qquad K_i \in \Omega_h . \tag{3.3}$$

We look for a solution to (3.1) in the finite element space

$$\mathcal{V}_h \stackrel{\text{def}}{=} \{ v \in L_2(\Omega) : v|_{K_i} \in H^p(K_i),\ \forall K_i \in \Omega_h \} . \tag{3.4}$$

Here $H^p(K_i)$ denotes the space of polynomials of degree at most p in n variables within the element K_i. Note that we are not imposing any continuity requirement for the solution between adjacent elements. The finite element solution to (3.1) can be written as

$$\widehat{p}^{(a,b)}_{x(t)\xi} = \sum_{i=1}^{N_{el}} \widehat{p}_i(a,b,t) , \qquad \widehat{p}_i(a,b,t) \stackrel{\text{def}}{=} \sum_{j=0}^{d} \alpha^j_{K_i}(t,b) \psi^j_{K_i}(a) , \tag{3.5}$$

where d denotes the number of degrees of freedom within each element K_i, and $\psi^j_{K_i}(a) \in H^p(K_i)$ $(j = 1, \ldots, d)$ is the set of basis functions in the element K_i. We substitute (3.5) into (3.1) and impose that the residual is orthogonal to the finite element space $\mathcal{V}_h$. By using the simplified notation $\widehat{p} = \widehat{p}^{(a,b)}_{x(t)\xi}$, this yields the following elementwise Galerkin formulation

$$\int_{K_i} q \frac{\partial \widehat{p}}{\partial t} da = \int_{K_i} \nabla_a q \cdot F[\widehat{p}] da - \int_{\partial K_i} q F[\widehat{p}] \cdot n_i dS , \qquad \forall q \in H^p(K_i) , \tag{3.6}$$

where n_i denotes the outward normal unit vector on the boundary ∂K_i. An important part of the solution process is the evaluation of the multidimensional flux $F[\widehat{p}]$ through the element boundary ∂K_i, i.e., the computation of the last integral in (3.6). Since we allowed discontinuous solutions across adjacent elements, the value of $F[\widehat{p}]$ is not

unique on ∂K_i. Therefore, we replace $F[\widehat{p}]$ with the *numerical flux* $\widetilde{F}[\widehat{p}_-, \widehat{p}_+]$, representing the information transferred through the boundary of adjacent elements. The quantities $\widehat{p}_-$ and $\widehat{p}_+$ here represent, respectively, the finite element solution within the element K_i and the solution within the adjacent ones. Among various schemes to compute the numerical flux $\widetilde{F}[\widehat{p}_-, \widehat{p}_+]$, we consider here the Roe scheme [48] (upwind flux), which is simple and is known to work well for advection dominated equations. Such a scheme can be explicitly written as

$$\widetilde{F}_j[\widehat{p}_-, \widehat{p}_+] = \begin{cases} F_j[\widehat{p}_-]\,, & \bar{a} \geq 0\,, \\ F_j[\widehat{p}_+]\,, & \bar{a} < 0\,, \end{cases} \qquad \bar{a} = \frac{F_j[\widehat{p}_+] - F_j[\widehat{p}_-]}{\widehat{p}_+ - \widehat{p}_-}\,,$$

where $\widetilde{F}_j$ $(j = 1, \ldots, n)$ denotes the component of the numerical flux along the direction a_j.

3.1.2. Adaptivity. The solution to the joint REPDF equation (3.1) can be supported over a very small region of the response phase space (see, e.g., Figure 1.1). In order to save computational resources and resolve accurately such local dynamics, we propose an adaptive algorithm that refines the computational grid where it is needed. Such h-type refinement can be based both on error estimates involving local variances or on particle methods. Hereafter, we discuss these two different approaches.

Adaptivity based on local variance and boundary flux difference. The error estimate presented in [34] for the DG discretization of the advection equation suggests that the error depends on the derivative of the solution as well on the amplitude of its jump at the element boundaries. This observation led us to develop a new adaptive criterion based on the boundary flux difference and the elementwise variance of the PDF. The basic idea of the variance criterion [63] is to split the finite element K_i whenever the following inequality is satisfied:

$$\sigma_{K_i} \mathcal{J}_{K_i} \geq \theta_1\,. \tag{3.7}$$

Here σ_{K_i} denotes the local standard deviation of the PDF in the element K_i while $\mathcal{J}_{K_i}$ is the relative element size. The threshold θ_1 can be selected appropriately, for example, with reference to the standard deviation of the PDF at the initial time. The procedure is illustrated in Figure 3.1 for finite elements in one and two dimensions, and it usually yields nonconforming grids such as those in Figure 4.6. In addition to the variance criterion, which is known to be insufficient for advection dominated equations [45], we have implemented another constraint, namely, a boundary flux difference controller

$$\int_{\partial K_i} |F[\widehat{p}_-] - F[\widehat{p}_+]|\, dS \geq \theta_2, \tag{3.8}$$

where we recall $\widehat{p}_-$ is the finite element solution in the element K_i while $\widehat{p}_+$ is the solution in the adjacent elements. If condition (3.8) is satisfied, then the element is split as in Figure 3.1.

The inverse operation, i.e., the merging of neighborhood elements, is based on the local variance criterion (3.7). In particular, we merge a group of elements with common boundaries if the summation of the local variances is small enough, i.e., less or equal than a threshold θ_3.

Adaptivity based on sample paths. An alternative criterion to refine the computational mesh in the phase space may be based on the analysis of a few sample

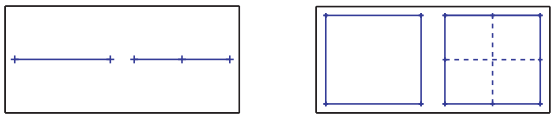

FIG. 3.1. *Mesh refinement in one- and two-dimensional phase spaces.*

trajectories of the stochastic dynamical system (2.1). The key idea is the following. We first sample a small ensemble of possible states of the system at time t according to the marginalized PDF

$$p^{(a)}_{x(t)} = \int_{\mathbb{R}^m} p^{(a,b)}_{x(t)\xi} db\,. \tag{3.9}$$

Then we evolve these states in time by integrating the system (2.1). Based on the analysis of the trajectories and on the concentration of samples in the phase space, we refine the computational mesh. The adaptive criterion is based on the relative number of samples within each finite element. If such number exceeds a prescribed threshold value θ_4 then the element is split as in Figure 3.1. A similar criterion is used to merge neighborhood elements. Once the adapted mesh has been identified, we interpolate the finite element solution (3.5) on the new mesh and solve the PDF equation (3.1) within the considered period of time. This procedure is illustrated in Figure 4.2, with reference to the dynamics of a stochastic nonlinear pendulum.

Validation of the variance/flux difference adaptive criterion. Let us consider the one-dimensional stochastic "decay" problem

$$\frac{\partial x\,(t;\omega)}{\partial t} = -x\,(t;\omega) + \sin(t) + \xi(\omega)\,, \qquad x\,(0;\omega) = x_0(\omega), \tag{3.10}$$

where $\xi(\omega)$ and $\eta(\omega)$ are zero-mean independent Gaussian random variables, both with variance $1/10$. The evolution equation for the joint REPDF (3.1) in this case reduces to

$$\frac{\partial p^{(a,b)}_{x(t)\xi}}{\partial t} = -\frac{\partial}{\partial a}\left[(-a + \sin(t) + b)\, p^{(a,b)}_{x(t)\xi}\right], \qquad t \geq 0, \quad a, b \in \mathbb{R}, \tag{3.11}$$

with initial condition

$$p^{(a,b)}_{x(0)\xi} = p^{(a)}_{x_0} p^{(b)}_{\xi} = \frac{5}{\pi} e^{-5(a^2+b^2)}\,. \tag{3.12}$$

The analytical solution to (3.11)–(3.12) can be obtained by using the method of characteristics [46], as

$$p^{(a,b)}_{x(t)\xi} = \frac{5e^t}{\pi} e^{-5[\widehat{\alpha}(a,b,t)^2+b^2]}\,,$$

where

$$\widehat{\alpha}(a,b,t) \stackrel{\text{def}}{=} e^t(a-b) + b - \frac{1}{2}\left[1 + e^t(\sin(t) - \cos(t))\right]. \tag{3.13}$$

Next, we consider the numerical simulation of (3.11) by using the proposed adaptive DG numerical scheme. The computational domain for the response variable a is chosen as $\Omega = [-1,\, 1]$ while the excitation variable b is assumed to be in $\mathbb{R}$. Also, the finite element space (3.4) is defined in terms of Legendre polynomials while a Gauss–

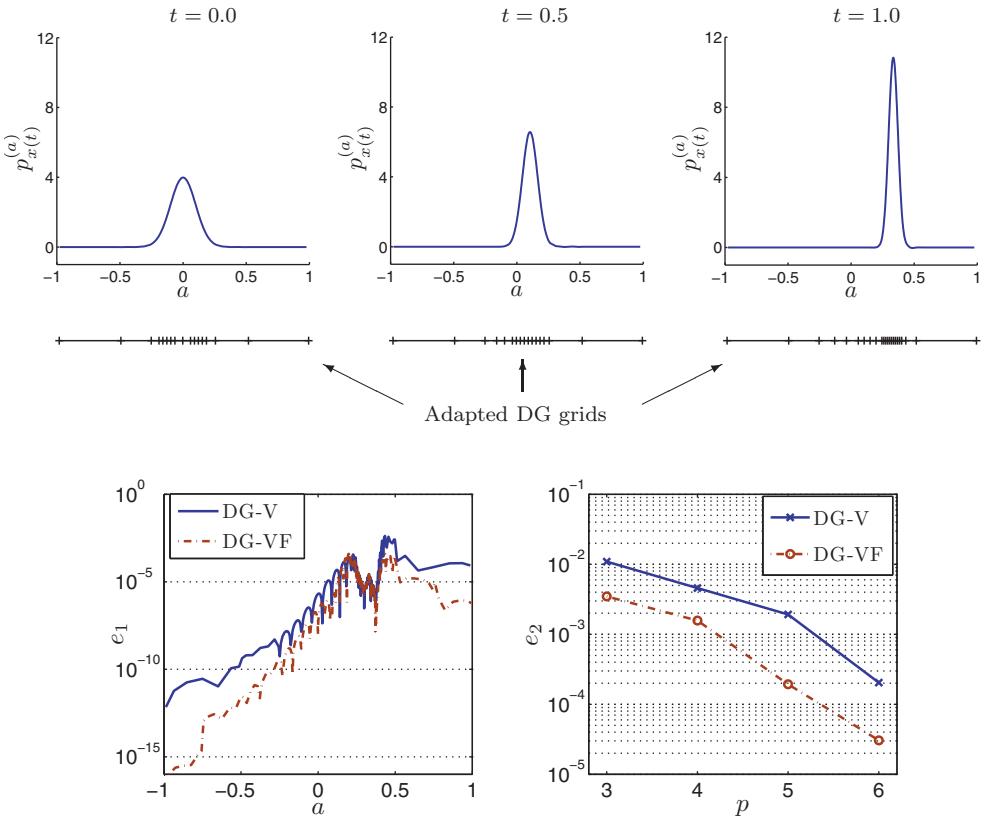

FIG. 3.2. *Time snapshots of the response probability of the decay problem as computed by the proposed adaptive DG method (first row). In the second row we plot the errors* (3.14) *and* (3.15) *between the DG solution and the analytical solution at the final time* $t = 1$. *Shown are the results of different adaptive strategies: DG-V (variance criterion), DG-VF (variance/flux difference criterion). We also show p-type convergence of* e_2.

Hermite collocation method with q points is considered for the variable b.[2] The time integration follows a fourth-order Runge–Kutta scheme with time step $\Delta t = 10^{-3}$. In Figure 3.2 we show the the numerically computed response probability of the system at different times together with the corresponding adapted mesh. In order to examine the accuracy of the DG solution relative to the analytical solution (3.1.2), we consider two different types of errors, namely, the absolute error

$$e_1(a,t) \stackrel{\text{def}}{=} \left| p^{(a)}_{x(t)} - \widehat{p}^{(a)}_{x(t)} \right| \tag{3.14}$$

and the mean-squared error

$$e_2(t) \stackrel{\text{def}}{=} \left[\int_{-1}^{1} \left(p^{(a)}_{x(t)} - \widehat{p}^{(a)}_{x(t)} \right)^2 da \right]^{1/2}. \tag{3.15}$$

These errors are exhibited in Figure 3.2 at $t = 1$, for the adaptive strategies based on the local variance criterion (3.7) and the local variance/boundary flux difference

[2]Thus, the total number degrees of freedom of the system is $N_{el}(p+1)q$, where N_{el} denotes the number of finite elements in Ω.

TABLE 3.1
Number of elements at $t = 1$ by using the variance (DG-V) and the variance/flux difference (DG-VF) adaptivity criteria. Shown are results for different polynomial orders p.

p	3	4	5	6
DG-V	37	37	37	37
DG-VF	62	49	41	41

criterion (3.8). The threshold parameters are set as $\theta_1 = 0.02$, $\theta_2 = 0.005/5^{\max\{p-3,0\}}$, and $\theta_3 = 0.001$ in this specific example. As can be seen in Figure 3.2 and Table 3.1 the local variance/boundary flux difference criterion performs substantially better than the local variance criterion, without increasing significantly the number of elements.

3.2. Excitation space. In most applications, we are interested in the response PDF of the system, i.e., in the multidimensional integral

$$p^{(a)}_{x(t)} = \int_{\mathbb{R}^m} p^{(a,b)}_{x(t)\xi} db\,, \tag{3.16}$$

with respect to the parameters $(b_1, \ldots, b_m)$. In order to compute such an integral, we use efficient cubature formulas with high polynomial exactness [17, 24, 41, 44]. In practice, we sample (3.1) with respect to the parameters b at appropriate quadrature or sparse grid points and then compute an approximation to the integral (3.16) in the form

$$\int_{\mathbb{R}^m} p^{(a,b)}_{x(t)\xi} db \simeq \sum_{k=1}^{q} w_k p^{\left(a,b^k\right)}_{x(t)\xi}\,, \quad b^k = (b^k_1, \ldots, b^k_m)\,, \tag{3.17}$$

where w_k are quadrature weights.

4. Numerical results. In this section we present numerical applications of the proposed adaptive DG method to different prototype stochastic problems involving randomly forced nonlinear oscillators.

4.1. Nonlinear pendulum. We study the stochastic dynamics of a nonlinear pendulum subject to an external random driving torque. A deterministic version of this problem has been studied in the past as a prototype problem to understand routes to chaos (see, e.g., [3, 14, 22]). In particular, we consider the following model equation

$$\frac{d^2\theta(t;\omega)}{dt^2} + \frac{d\theta(t;\omega)}{dt} + \kappa \sin\left(\theta(t;\omega)\right) = h(t;\omega)\,, \tag{4.1}$$

where θ denotes the position of the pendulum, $\kappa \sin(\theta)$ is the restoring torque, and $h(t;\omega)$ is an external random driving torque with prescribed statistical properties. Equation (4.1) can be written as a first-order system as

$$\begin{cases} \dfrac{dx_1(t;\omega)}{dt} = x_2(t;\omega)\,, \\ \dfrac{dx_2(t;\omega)}{dt} = -x_2(t;\omega) - \kappa \sin\left(x_1(t;\omega)\right) + h(t;\omega)\,, \end{cases} \tag{4.2}$$

where $x_1(t;\omega) = \theta(t;\omega)$ and $x_2(t;\omega) = d\theta(t;\omega)/dt$. We assume that we have available a Karhunen–Loève representation external random torque in the form

$$h(t;\omega) = \sum_{k=1}^{m} \xi_k(\omega) h_k(t), \tag{4.3}$$

where $\{\xi_k(\omega)\}$ is a set of uncorrelated random variables with known joint PDF, and $h_k(t)$ are unnormalized eigenfunctions of the autocorrelation of $h(t;\omega)$. By using the method discussed in section 2, it is straightforward to obtain the evolution equation for the joint PDF of the vector $\{x_1(t;\omega), x_2(t;\omega)), \xi_1(\omega), \ldots, \xi_m(\omega)\}$,

$$p^{(a,b)}_{x(t)\xi} \overset{\text{def}}{=} p^{(a_1,a_2,b_1,\cdots,b_m)}_{x_1(t)x_2(t)\xi_1\cdots\xi_m} = \left\langle \delta(a_1 - x_1)\delta(a_2 - x_2) \prod_{k=1}^{m} \delta(b_k - \xi_k) \right\rangle , \tag{4.4}$$

where the average is with respect to the joint PDF of $\{\xi_k(\omega)\}$ and the initial state $\{x_1(t_0;\omega), x_2(t_0;\omega)\}$. The kinetic equation has the form (2.3) with

$$\mathcal{L}(t) = -a_2 \frac{\partial}{\partial a_1} + \mathcal{I} + \left(a_2 + \kappa \sin(a_1) - \sum_{k=1}^{m} b_k h_k(t) \right) \frac{\partial}{\partial a_2} . \tag{4.5}$$

In particular, let us consider here the simple case where the random torque $h(t;\omega)$ depends only on one Gaussian random variable ξ_1, i.e.,

$$h(t;\omega) = \xi_1(\omega) \sin(10t) . \tag{4.6}$$

We set the parameter κ in (4.1) as $\kappa = 40$. This leads us to the PDF equation

$$\frac{\partial p^{(a,b)}_{x(t)\xi}}{\partial t} = -\frac{\partial}{\partial a_1} \left(a_2 p^{(a,b)}_{x(t)\xi} \right) + \frac{\partial}{\partial a_2} \left(\left[a_2 + 40 \sin(a_1) - b_1 \sin(10t) \right] p^{(a,b)}_{x(t)\xi} \right) . \tag{4.7}$$

The initial condition $(x_1(0;\omega), x_2(0;\omega))$ is assumed to be jointly Gaussian and independent from the variable ξ_1 in (4.6). Specifically, the joint PDF of x_1 (position), x_2 (momentum), and ξ_1 at the initial time $t_0 = 0$ is set as

$$p^{(a,b)}_{x(0)\xi} = \frac{4}{3(2\pi)^{3/2}} \exp\left[-\frac{8}{9} \left(a_1 - \frac{4}{5}\pi \right)^2 - 2a_2^2 - \frac{b_1^2}{2} \right] . \tag{4.8}$$

This system physically corresponds to a dissipative nonlinear pendulum dropped from a random initial position near the unstable vertical one, with a random velocity. Note that the mean initial position is not exactly vertical, but it is set at $\langle x_1 \rangle = 4\pi/5$, i.e., on the right semi-half of the circle (see the sketch in Figure 4.1(a)). Several realizations of the time evolution of this system are shown in Figure 4.1(b)–(c). It is seen that the pendulum never makes a complete rotation, but it simply falls to the lower vertical position through half rotations and then it keeps oscillating around it due to the sinusoidal driving torque. Specifically, the clockwise half rotation leads to oscillations near $x_1 = 0$, while the counterclockwise half rotation leads to oscillations near $x_1 = 2\pi$. Although these two quasi-equilibrium configurations represent the same physical state, they are reached through different paths, i.e., clockwise or counterclockwise rotations. Thus, the continuous ensemble of initial conditions is split into two disjoint ensembles in a finite time. This leads to a particular type of discontinuity in the probability space that cannot be resolved by using standard polynomial chaos (see, e.g., [62]), or global probabilistic collocation. Extensions such as ME-gPC [64] or ME-PCM [17] can resolve this discontinuity.

In Figure 1.1 we compare the DG results of the PDF equation (4.7) with several time snapshots of the sample phase space. We have chosen polynomial order $p = 5$ for the response space elements, $q = 9$ collocation points for the excitation space,

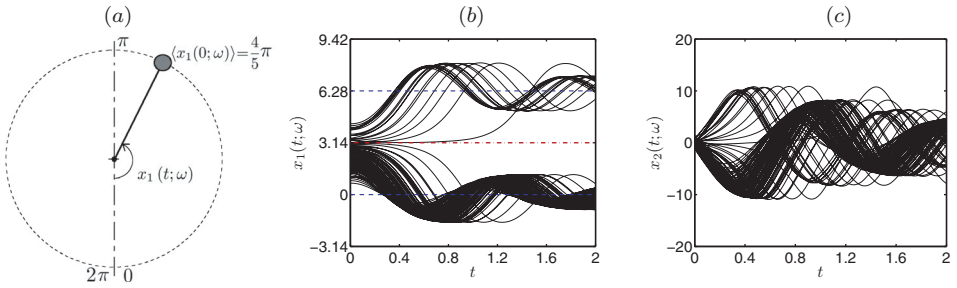

FIG. 4.1. (a) *Sketch of pendulum, illustrating the mean initial position. In* (b) *and* (c) *we show the temporal dynamics of several sample paths of the position and the velocity, respectively.*

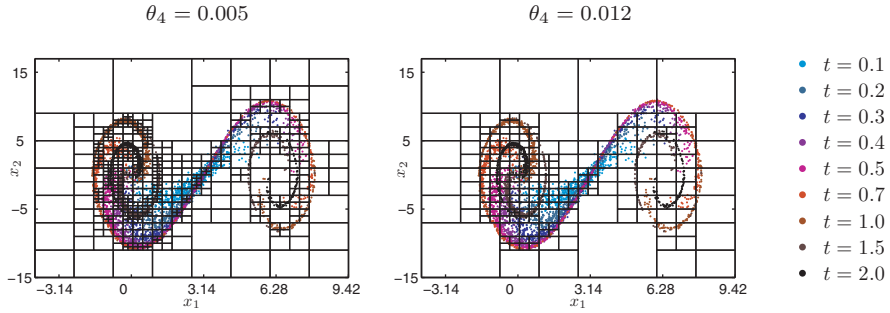

FIG. 4.2. *Sample phase plane of the pendulum at several time steps t and nonconforming grid based on the entire sample path $t \in [0, 2]$. Shown are results for different values of adaptive parameter θ_4.*

and fourth-order Runge–Kutta scheme for the time integration, with time step $\Delta t = 5 \cdot 10^{-4}$. The adapted nonconforming mesh shown in Figure 4.2 is generated by using the adaptivity criterion based on sample paths discussed in section 3.1.2. The threshold for the relative number of particles in each element is set to $\theta_4 = 0.005$ (see Figure 4.2(a)). An analysis of Figure 1.1 shows that the symmetry of the system is broken by setting the mean initial position of the pendulum to $\langle x_1(0,\omega)\rangle = 4\pi/5$. In fact, a larger portion of the phase space evolves towards the quasi-equilibrium state through a clockwise rotation. In turn, this leads to a bimodal PDF, with accumulation near $x_1 = 0$, as demonstrated in Figure 4.3. The effects of the adaptive threshold θ_4 on the response PDF of the system are shown in Figure 4.4. It is seen that despite the robustness of the adaptive grid generation criterion, a proper selection of the threshold parameter is necessary for accurate results.

We emphasize that the numerical simulation of the REPDF equation (4.7) based on global expansion bases, such as Fourier spectral methods, would require a very high resolution to represent accurately the REPDF within the response domain $\Omega = [-4/3\pi, 3\pi] \times [-15, 17]$.

Non-Gaussian random coefficient and random forcing. Non-Gaussian random fields can be easily adopted in the REPDF approach. We consider two different examples, using a non-Gaussian random coefficient and a non-Gaussian random field as the forcing term. We first take $\kappa(\omega)$ as a uniform random variable on the interval [20, 30]. In addition, we choose $h(t;\omega)$ to be an exponentially correlated random field expanded by using the Karhunen–Loève series in terms of uniform random variables. We note

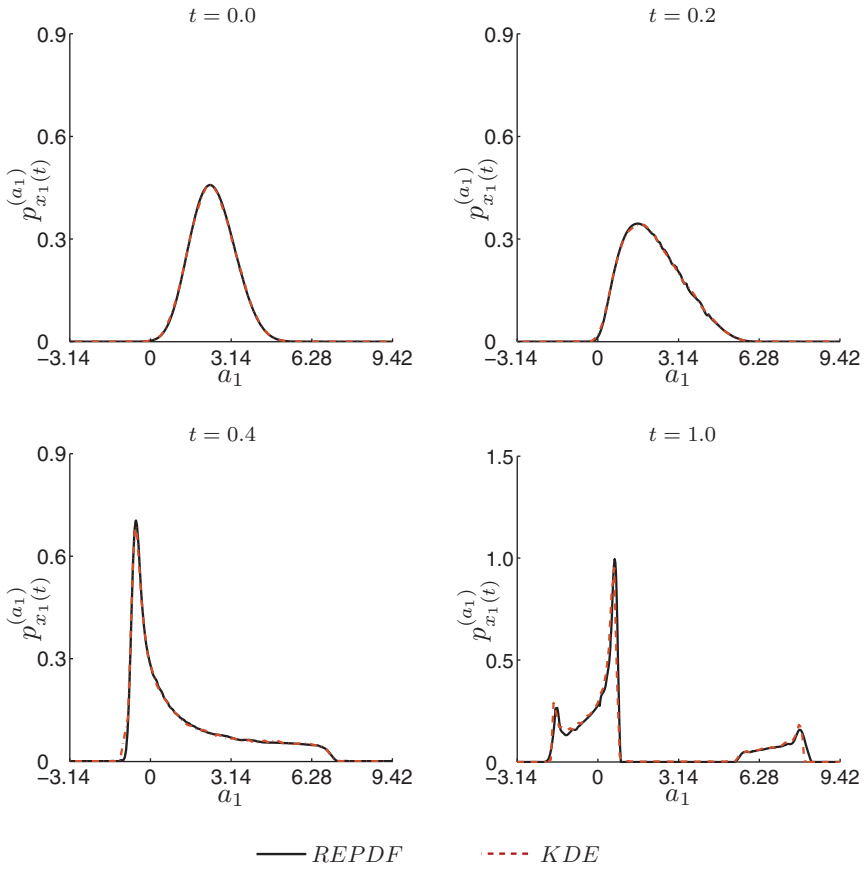

FIG. 4.3. *Comparison between the PDF of position of the pendulum $x_1(t;\omega)$ as computed by the proposed adaptive DG method (continuous line: REPDF) and an accurate nonparametric kernel estimation method based on* 50000 *samples (dashed line: KDE). Shown are results at different times.*

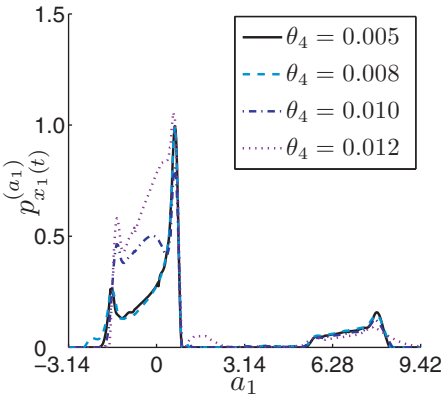

FIG. 4.4. *Effects of the adaptive threshold θ_4 on the response PDF of the system at time $t = 1$. The nonconforming grids corresponding to $\theta_4 = 0.005$ and $\theta_4 = 0.012$ are shown in Figure* 4.2.

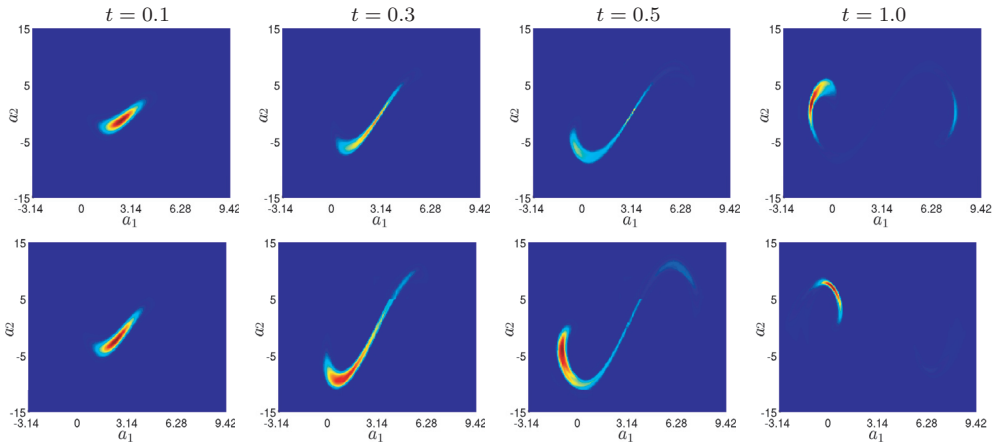

FIG. 4.5. *Evolution of the joint PDF of the position and the momentum of the pendulum with uniform random coefficient (top) and exponentially correlated non-Gaussian random forcing (bottom) at different times.*

that the PDF of the superimposition of a finite number of independent uniform random variables is quite complicated and the references can be found in [50]. Particularly, we take $\langle h(t;\omega)\rangle = 5.0$ and the covariance function as $e^{-|t-s|}$ (see [30] for analytical expressions). In both cases, the uniform random variables are simulated with 9 Legendre collocation points in each dimension and the computed solutions are plotted in Figure 4.5 up to $t = 1.0$. Compared to the Gaussian example in Figure 1.1, the PDFs are less concentrated due to the larger variance of the uniform random variables.

4.2. Duffing oscillator. Many physically interesting phenomena involving nonlinear oscillations can be modeled in terms of the stochastic Duffing equation

$$\begin{cases} \dfrac{dx_1(t;\omega)}{dt} = x_2(t;\omega)\,, \\ \dfrac{dx_2(t;\omega)}{dt} = -\gamma x_2(t;\omega) - \kappa x_1(t;\omega) - \beta x_1(t;\omega)^3 + f(t;\omega)\,, \end{cases} \tag{4.9}$$

where $f(t;\omega)$ is a random forcing term. We assume that the initial condition of the system (4.9) is jointly Gaussian with mean (μ_1, μ_2), variance (σ_1, σ_2), and cross correlation σ_{12}. From the point of view of modern dynamical systems theory [25], the ensemble of solutions to (4.9) is very rich, and it has been subjected to extensive analytical and numerical investigation [5, 16, 37, 67]. The statistical properties of the random forcing term $f(t;\omega)$ also play a fundamental role in the development of the stochastic dynamics. Hereafter we consider different examples involving low-dimensional as well as high-dimensional random forcing terms. In all cases, the PDF equation is solved numerically by using the proposed spectral DG method with elementwise polynomial order $p = 4$ in the response space, $q = 15$ collocation points in the excitation space, and a fourth-order Runge–Kutta scheme for the time integration. The initial time step is set to $\Delta t = 10^{-3}$ and it is adaptively adjusted whenever it violates the CFL condition [12],

$$\frac{\Delta t}{\Delta a_1}\frac{d\mathcal{F}_1}{dp} + \frac{\Delta t}{\Delta a_2}\frac{d\mathcal{F}_2}{dp} < \frac{1}{2p+1}\,. \tag{4.10}$$

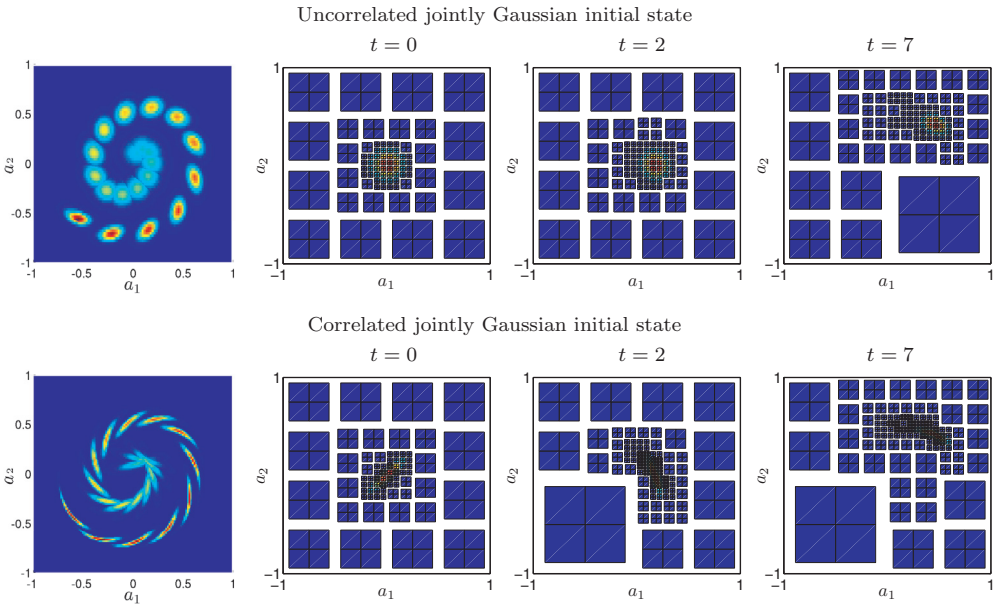

FIG. 4.6. *Time snapshots of the response PDF of the Duffing system and corresponding adapted grids obtained by using the local variance/flux difference criterion. Shown are also the effects of the correlation σ_{12} between the initial position x_1 and the momentum x_2 of the oscillator: First row: $\sigma_{12} = 0.0$ (uncorrelated); Second row: $\sigma_{12} = 0.09$ (correlated).*

The grid adaptivity is based on the local variance/boundary flux difference criterion (see section 3.1.2) with parameters $\theta_1 = 0.2 \min(\sigma_1, \sigma_2)$, $\theta_2 = 0.04$, and $\theta_3 = 0.001$.

Stable oscillations and chaotic motion. The ensemble of solutions to the Duffing equation (4.9) includes stable oscillations and chaotic motion, depending on the system parameters [5]. We first test our adaptive DG method on a stable manifold of periodic states. To this end, we set the damping and the stiffness coefficients in (4.9) and (4.15) to $\gamma = 0.1$, $\kappa = 1.0$, and $\beta = 1.0$ and consider a deterministic-type forcing $f(t) = D\cos(t)$. This yields the following kinetic equation governing the response PDF,

$$\frac{\partial p^{(a)}_{x(t)}}{\partial t} = -\frac{\partial}{\partial a_1}\left(a_2\, p^{(a)}_{x(t)}\right) - \frac{\partial}{\partial a_2}\left(\left[-\gamma a_2 - \kappa\, a_1 - \beta a_1^3 + D\cos(t)\right] p^{(a)}_{x(t)}\right). \tag{4.11}$$

The initial condition is jointly Gaussian with parameters $\mu_{1,2} = 0.0$, $\sigma_{1,2} = 0.1$, and variable correlation σ_{12}.

The time dynamics of the response PDF of the Duffing system is shown in Figure 4.6 for initial conditions with different correlation coefficients and $D = 0.2$. We notice that the dynamics corresponding to uncorrelated initial state remains smooth and it follows a stable oscillating motion. On the contrary, the dynamics corresponding to a correlated initial state becomes steeper and more skewed as time goes on. The adapted grids generated by the variance/flux difference criterion correctly follow the peak locations of the PDF, allowing us to resolve the dynamics accurately at a reasonable computational cost. The number of nonconforming finite elements produced by the variance/flux difference adaptive procedure is shown in Figure 4.7 versus time for different choices of θ_1 and θ_2. In the same figure we also exhibit

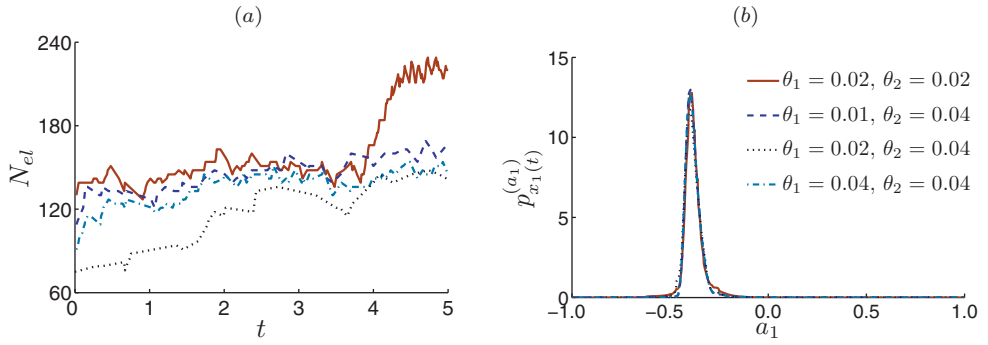

FIG. 4.7. (a) *Number of elements N_{el} generated by the variance/flux difference adaptive criterion versus time. Shown are results obtained by using different thresholds θ_1 and θ_2 and a jointly Gaussian initial PDF with correlation $\sigma_{12} = 0.09$ (see Figure* 4.6*).* (b) *Effects of the thresholds on the PDF of $x_1(t;\omega)$ at time $t = 5$.*

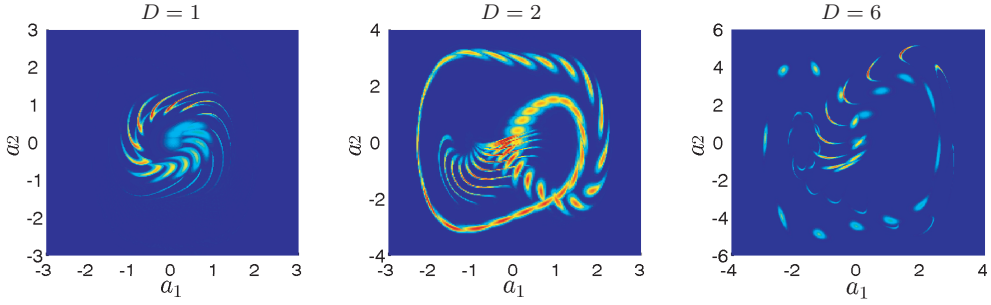

FIG. 4.8. *Route to chaos in the response PDF of the Duffing oscillator when the amplitude of D, the forcing, is increased in* (4.15) *from $D = 1$ (system with negative Lyapunov exponent) to $D = 6$ (system with positive Lyapunov exponent). Shown are time snapshots of the response PDF evolving from a jointly Gaussian and uncorrelated initial state.*

the effects of such thresholds on the PDF of $x_1(t;\omega)$ at time $t = 5$. It is seen that, differently from the sample-path based adaptive technique previously discussed, the variance/flux difference procedure is not very sensitive to the selection of the threshold parameters.

We remark that if we would have used uniform grids, the number of elements would be from *four to twenty times higher* than ours, at a comparable level of accuracy. Next, we consider more complicated stochastic dynamics, such as chaotic motions. To this end, we set $\kappa = 0.0$, $\gamma = 0.1$, $\beta = 0.1$ in (4.9) and (4.11). It is known that this system undergoes several transitions as a function of the parameter D (amplitude of the forcing). In particular, the phase diagrams obtained by Bonatto, Gallas, and Ueda in [5] clearly show that within the range $D \in [0, 6]$ we have solutions with negative Lyapunov exponents (regular) as well as solutions with positive Lyapunov exponents (chaotic). This is demonstrated in Figure 4.8, where we show the time snapshots of the response PDF of the system for different values of D. It is seen that the dynamics of the PDF, which is accurately captured by the proposed adaptive DG method, gradually loses its regularity when D is increased from 1 to 6.

This onset of chaos at $D \simeq 5$ can be also appreciated in Figure 4.9 where we plot the evolution of the joint REPDF obtained by marginalizing the solution to the

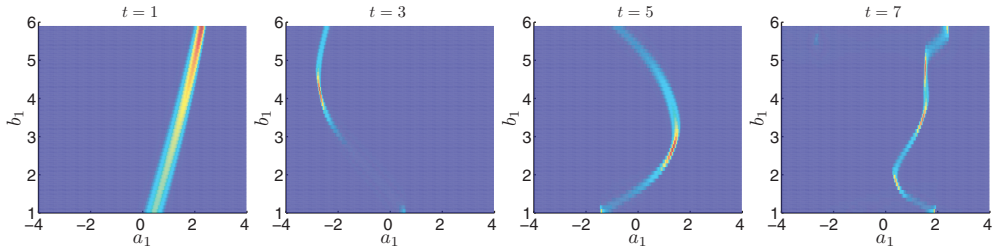

FIG. 4.9. *Joint REPDF of $x(t;\omega)$ and $\xi(\omega)$ (random amplitude of the forcing) at different times. The onset of chaos $\xi(\omega) \simeq 5$ and the chaotic region $\xi(\omega) \in [5,6]$ can be appreciated at time $t = 7$, where the PDF is scattered within the region $b_1 \in [5,6]$.*

kinetic equation

$$\frac{\partial p^{(a,b)}_{x(t)\xi}}{\partial t} = -\frac{\partial}{\partial a_1}\left(a_2\, p^{(a,b)}_{x(t)\xi}\right) - \frac{\partial}{\partial a_2}\left(\left[-\gamma a_2 - \kappa\, a_1 - \beta a_1^3 + b_1\cos(t)\right] p^{(a,b)}_{x(t)\xi}\right), \tag{4.12}$$

with respect to a_2. This equation corresponds to a random forcing in the form $f(t;\omega) = \xi(\omega)\cos(t)$, where $\xi(\omega)$ is a uniform random variable in $[0,6]$. The results of Figure 4.9 show that at $t = 7$ the joint REPDF is scattered within the region $b_1 \in [5,6]$. This indicates a possible chaotic scenario which is consistent with the phase diagrams obtained in [5].

Colored random noise. We address here the question of whether the joint response-excitation approach can provide an effective computational tool to simulate the effects of colored random noise in physical systems. To this end, we model the forcing term in (4.9) as an exponentially correlated Gaussian random process satisfying

$$\langle f(t;\omega)\rangle = 0, \qquad \langle f(t;\omega) f(s;\omega)\rangle = \frac{D}{\tau} e^{-\frac{|t-s|}{\tau}}, \tag{4.13}$$

where $D > 0$ denotes the amplitude of the noise. The autocorrelation of f can be made arbitrarily close to a Dirac delta function by sending the *correlation time* τ to zero.[3] We expand the process $f(t;\omega)$ in a finite-dimensional Karhunen–Loève series as

$$f(t;\omega) = \left(\frac{D}{\tau}\right)^{1/2} \sum_{k=1}^{m} \sqrt{\lambda_k} e_k(t)\xi_k(\omega), \quad t \in [0,\, T], \tag{4.14}$$

where $\xi_k(\omega)$ are uncorrelated normal random variables, while λ_k and $e_k(t)$ are, respectively, the eigenvalues and the eigenfunctions of the exponential correlation function $\exp(-|t-t'|/\tau)$ (see [30] for analytical expressions).

The effects of the correlation time τ on the dimensionality m of the Karhunen–Loève series (4.14) are reported in Table 4.1. It is seen that processes with a small correlation time are high dimensional, i.e., they depend on many random variables. As a consequence, the kinetic equation for the joint REPDF of the system can be high dimensional as well. In fact, we obtain

$$\frac{\partial p^{(a,b)}_{x(t)\xi}}{\partial t} = -\frac{\partial}{\partial a_1}\left(a_2\, p^{(a,b)}_{x(t)\xi}\right) - \frac{\partial}{\partial a_2}\left(\left[-\gamma a_2 - \kappa\, a_1 - \beta a_1^3 + \sum_{k=1}^{m} f_k(t) b_k\right] p^{(a,b)}_{x(t)\xi}\right), \tag{4.15}$$

[3] In fact, $\exp(-|t-t'|\tau)/\tau$ is an element of a delta sequence [32], converging to $2\delta(t-t')$ as $\tau \to 0$.

TABLE 4.1
Effects of the correlation time τ on the dimensionality of the Karhunen–Loève series (4.14). *The energy cutoff is set at 95% of the total energy of the process.*

τ	50.0	5.0	2.0	1.0	0.5	0.1	0.01
m	1	5	9	13	25	48	57

where we have defined

$$f_k(t) \stackrel{\text{def}}{=} \left(\frac{D\lambda_k}{\tau}\right)^{1/2} e_k(t)\,. \tag{4.16}$$

Equation (4.15) is a linear transport PDE in two phase variables (a_1, a_2) and m parameters $(b_1, \ldots, b_m)$, i.e., its solution at time t lies in an $(m+2)$-dimensional manifold.

White and weakly colored Gaussian random noise. In the limit of zero correlation time τ, the exponentially correlated Gaussian random process (4.14) becomes Gaussian white noise of magnitude $\sqrt{2D}$. In this case the dynamics of the response PDF of the system is governed by the Fokker–Planck equation [47]:

$$\frac{\partial p^{(a)}_{x(t)}}{\partial t} = -\frac{\partial}{\partial a_1}\left(a_2 p^{(a)}_{x(t)}\right) - \frac{\partial}{\partial a_2}\left(g(a_1,a_2)p^{(a)}_{x(t)}\right) + D\frac{\partial^2 p^{(a)}_{x(t)}}{\partial a_2^2}, \tag{4.17}$$

where $g(a_1, a_2) \stackrel{\text{def}}{=} -\gamma a_2 - \kappa a_1 - \beta a_1^3$. The second-order diffusion term is induced by the white noise forcing. A similar theory holds for weakly colored Gaussian random noise, In fact, by using the small correlation time approximation of the Furutsu–Novikov relation [19, 26, 27, 60], it is possible to obtain

$$\begin{aligned}\frac{\partial p^{(a)}_{x(t)}}{\partial t} =& -\frac{\partial}{\partial a_1}\left[a_2\, p^{(a)}_{x(t)}\right] - \frac{\partial}{\partial a_2}\left[g(a_1,a_2)p^{(a)}_{x(t)}\right] \\ &+ \frac{\partial^2}{\partial a_2 \partial a_1}\left[\frac{D}{\sqrt{\rho}}\left(\frac{1-e^{(\Lambda_1-1/\tau)t}}{1-\Lambda_1\tau} - \frac{1-e^{(\Lambda_2-1/\tau)t}}{1-\Lambda_2\tau}\right)p^{(a)}_{x(t)}\right] \\ &+ \frac{\partial^2}{\partial a_2^2}\left[\frac{D}{\sqrt{\rho}}\left(\frac{\Lambda_1(1-e^{(\Lambda_1-1/\tau)t})}{1-\Lambda_1\tau} - \frac{\Lambda_2(1-e^{(\Lambda_2-1/\tau)t})}{1-\Lambda_2\tau}\right)p^{(a)}_{x(t)}\right],\end{aligned} \tag{4.18}$$

where

$$\rho \stackrel{\text{def}}{=} \gamma^2 + 4(\kappa + 3\beta a_1^2)\,, \quad \Lambda_1 \stackrel{\text{def}}{=} \frac{-\gamma+\sqrt{\rho}}{2}\,, \quad \Lambda_2 \stackrel{\text{def}}{=} \frac{-\gamma-\sqrt{\rho}}{2}\,. \tag{4.19}$$

The kinetic equation (4.18) holds for exponentially correlated Gaussian random forcing terms with very small correlation time τ, and it can be considered as a first-order correction to the Fokker–Planck equation (4.17), namely, the effective Fokker–Planck (EFKP) equation.

The intermediate range of correlation times is unfortunately not easily accessible by using correlation time expansions. In fact, the numerical solution to the classical EFKP equation (4.18) for the case $\tau = 1$ becomes unstable after $t \geq 3$, indicating that $\tau = 1$ is beyond the convergence radius of the small correlation time approximation.

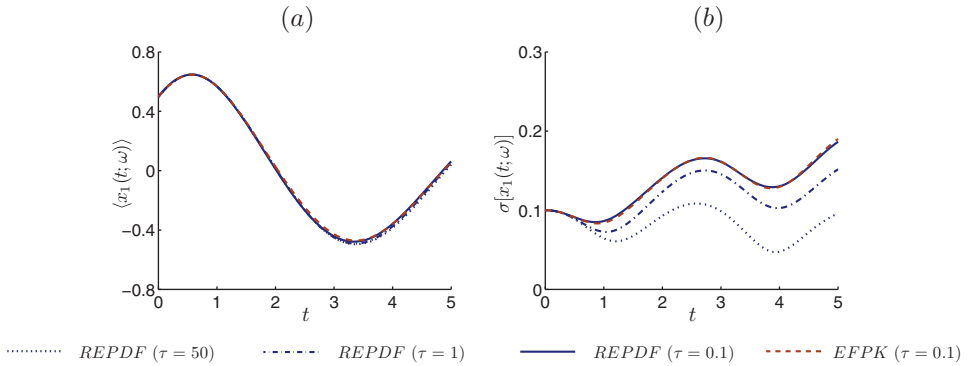

FIG. 4.10. *Mean* (a) *and standard deviation* (b) *of the solution to Duffing system for exponentially correlated Gaussian random forcing with different correlation times* τ. *The statistical properties plotted in* (a) *and* (b) *are obtained by computing moments of the PDF solving the joint REPDF equation* (4.15) *and the EFPK equation* (4.18); *the moments for* $\tau = 0.1$ *agree with each other.*

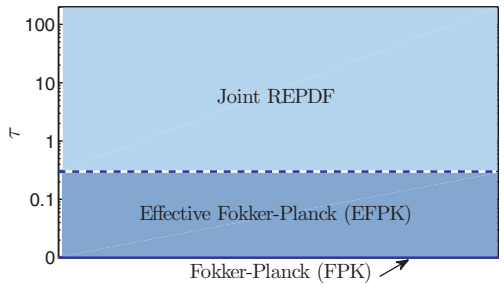

FIG. 4.11. *The appropriate approach for different values of* τ, *where we emphasize that the REPDF equation extends the classical PDF approaches and enables us to simulate the whole range of correlation time.*

This leads us to investigate the consistency of the response-excitation approach with the classical EFPK theory for weakly correlated random forcing. This is done in Figure 4.10 where we compare the mean and the standard deviation of the solution to the Duffing equation driven by random noise with different correlation times τ. These statistical moments are obtained by integrating the solution to the PDF equations (4.18) and (4.15). It is seen that for $\tau = 0.1$ the response-excitation approach[4] is consistent with the classical EFKP approach. Moreover, we propose an appropriate approach to simulate the stochastic system excited by different values of correlation time τ in Figure 4.11 and emphasize that the REPDF approach enables us to simulate the whole range of correlation times. The effects of τ on the temporal dynamics of response PDF are exhibited in Figure 4.12. It is seen that random noise with a small correlation time (cases $\tau = 0.1$ and $\tau = 1.0$) induces a diffusion phenomenon in the PDF. On the other hand, for larger correlation times (case $\tau = 2$), the diffusion seems to be absent, and the maximum value of the response PDF increases with time.

[4]The dimensionality of the random forcing (4.14) is $m = 13$ for $\tau = 1.0$ and $m = 48$ for $\tau = 0.1$ (see Table 4.1). This means that the excitation space is 13 or 48 dimensional.

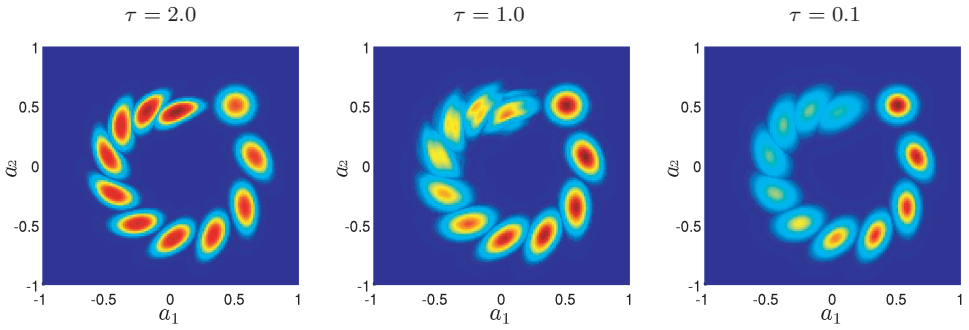

FIG. 4.12. *Time snapshots of the response PDF of the Duffing system for random noise with different correlation times τ. The initial condition in all cases is jointly Gaussian with mean $\mu_{1,2} = 0.5$.*

5. Summary. In this paper we have addressed the question of whether the joint REPDF approach can provide an effective computational tool to simulate the effects of *colored random noise in dynamical systems*. To this end, we have developed a nonconforming adaptive DG method for the joint REPDF equation governing the dynamics of an arbitrary nonlinear system with parametric-type uncertainty. Such a generalized PDF equation can be high dimensional as it can arise, for example, from a discretization of an SPDE subject to random boundary conditions, random initial conditions or random forcing. We have proposed different techniques to deal with high-dimensionality and possible discontinuities of the PDF solution in the response-excitation space. In particular, we have combined sparse grid and multi-element collocation approaches (excitation space) with a novel adaptive discontinuous Galerkin method (response space). The effectiveness of the proposed new algorithm has been demonstrated in two prototype applications dealing with the statistical properties of the randomly forced nonlinear pendulum and the stochastic Duffing oscillator. The same procedure can be readily extended to the joint REPDF equations corresponding to first-order SPDEs [59].

Further developments of the proposed methodology can be addressed along different directions. With reference to DG methods for PDF equations, more sophisticated numerical fluxes and limiters can be considered to obtain stronger conservative properties and preserve the positivity of the solution [28, 70]. The dimensionality of the response-excitation space is still the major issue underlying the joint REPDF equation, despite recent advances in numerical methods for high-dimensional systems such as PGD [8, 35, 42], ME-PCM [18], or ANOVA [6, 57, 68]. Nonetheless, some closure approximations to obtain the response PDF equation exist. As shown in section 4.2, the EFKP approximation can be applied for systems excited by a weakly correlated Gaussian random process. However, the range of applicability of the EFKP approach, that is, the transition value of τ between the REPDF and the EFKP in Figure 4.11 needs to be further investigated in different examples. Alternatively, some preliminary results using a moving kernel approach for the transient state and the Gaussian kernel approximation for long-time, steady-state closure can be found in [2, 51]. For high dimensionality in the response space, the second-order ANOVA expansion of the joint REPDF could lead to a reduction of the REPDF equation (2.3) into a coupled system of two-dimensional equations, which can be solved by using the adaptive DG method presented in this paper. Another approach to overcome the dimensionality problem in probability space can be based on a goal-oriented projection operator

framework of Zwanzig-type [10, 13]. This latter approach may allow us to determine exact PDF equations for low-dimensional nonlinear functionals of the solution to high-dimensional stochastic problems. Based on this formulation, one can avoid the integration of the full stochastic system and solve directly for the PDF of the low-dimensional functional of interest.

REFERENCES

[1] L. Arnold, *Random Dynamical Systems*, Springer Monogr. Math., Springer, Berlin, 2003.

[2] G. A. Athanassoulis, I. C. Tsantili, and Z. G. Kapelonis, *The joint response-excitation PDF evolution equation. Numerical solutions for the long-time, steady-state response of a half oscillator*, in Proceedings of the 11th ASCE Joint Specialty Conference on Probabilistic Mechanics and Structural Reliability, Notre Dame, IN, 2012.

[3] J. A. Blackburn, Z. Yang, S. Vik, H. J. T. Smith, and M. A. H. Nerenberg, *Experimental study of chaos in a driven pendulum*, Phys. D, 26 (1987), pp. 385–395.

[4] S. Blanes, F. Casas, J. A. Oteo, and J. Ros, *The Magnus expansion and some of its applications*, Phys. Rep., 470 (2009), pp. 151–238.

[5] C. Bonatto, J. A. C. Gallas, and Y. Ueda, *Chaotic phase similarities and recurrences in a damped-driven Duffing oscillator*, Phys. Rev. E, 77 (2008), 026217.

[6] Y. Cao, Z. Chen, and M. Gunzburger, *ANOVA expansions and efficient sampling methods for parameter dependent nonlinear PDEs*, Int. J. Numer. Anal. Model., 6 (2009), pp. 256–273.

[7] J.-B. Chen and J. Li, *A note on the principle of preservation of probability and probability density evolution equation*, Probab. Engrg. Mech., 24 (2009), pp. 51–59.

[8] F. Chinesta, A. Ammar, and E. Cueto, *Recent advances and new challenges in the use of the proper generalized decomposition for solving multidimensional models*, Arch. Comput. Methods. Appl. Mech. Engrg., 17 (2010), pp. 327–350.

[9] A. V. Chizhov and L. J. Graham, *Efficient evaluation of neuron populations receiving colored-noise current based on a refractory density method*, Phys. Rev. E, 77 (2008), 011910.

[10] A. J. Chorin, O. H. Hald, and R. Kupferman, *Optimal prediction and the Mori-Zwanzig representation of irreversible processes*, Proc. Natl. Acad. Sci. USA, 97 (2000), pp. 2968–2973.

[11] B. Cockburn, G. E. Karniadakis, and C.-W. Shu, *Discontinuous Galerkin methods*, Lect. Notes Comput. Sci. Eng. 11, Springer, Berlin, 2000.

[12] B. Cockburn and C.-W. Shu, *Runge-Kutta discontinuous Galerkin methods for convection dominated problems*, J. Sci. Comput., 16 (2001), pp. 173–261.

[13] E. Darve, J. Solomon, and A. Kia, *Computing generalized Langevin equations and generalized Fokker-Planck equations*, Proc. Natl. Acad. Sci. USA, 106 (2009), pp. 10884–10889.

[14] D. D'Humieres, M. R. Beasley, B. A. Huberman, and A. Libchaber, *Chaotic states and routes to chaos in the forced pendulum*, Phys. Rev. A (3), 26 (1982), pp. 3483–3496.

[15] B. G. Dostupov and V. S. Pugachev, *The equation for the integral of a system of ordinary differential equations containing random parameters*, Automat. Telemekh., 18 (1957), pp. 620–630 (in Russian).

[16] M. I. Dykman, R. Mannella, P. V. E.McClintock, F. Moss, and S. M. Soskin, *Spectral density of fluctuations of a double-well Duffing oscillator driven by white noise*, Phys. Rev. A (3), 37 (1988), pp. 1303–1313.

[17] J. Foo and G. E. Karniadakis, *The multi-element probabilistic collocation method (ME-PCM): Error analysis and applications*, J. Comput. Phys., 227 (2008), pp. 9572–9595.

[18] J. Foo and G. E. Karniadakis, *Multi-element probabilistic collocation method in high dimensions*, J. Comput. Phys., 229 (2010), pp. 1536–1557.

[19] R. F. Fox, *Functional-calculus approach to stochastic differential equations*, Phys. Rev. A (3), 33 (1986), pp. 467–476.

[20] R. F. Galán, *Analytical calculation of the frequency shift in phase oscillators driven by colored noise: Implications for electrical engineering and neuroscience*, Phys. Rev. E (3), 80 (2009), 036113.

[21] R. G. Ghanem and P. D. Spanos, *Stochastic Finite Elements: A Spectral Approach*, Springer-Verlag, New York, 1991.

[22] M. Gitterman, *The Noisy Oscillator: The First Hundred Years, from Einstein Until Now*, World Scientific, Hackensack, NJ, 2005.

[23] D. S. Goldobin, J. N. Teramae, H. Nakao, and G. B. Ermentrout, *Dynamics of limit-cycle oscillators subject to general noise*, Phys. Rev. Lett., 105 (2010), 154101.

[24] M. Griebel, *Sparse grids and related approximation schemes for higher dimensional problems*, in Foundations of Computational Mathematics, Santander 2005, L. M. Pardo, A. Pinkus, E. Süli, and M. J. Todd, eds., Cambridge University Press, Cambridge, 2006, pp. 106–161.
[25] J. Guckenheimer and P. Holmes, *Nonlinear oscillation, dynamical systems, and bifurcations of vector fields*, Appl. Math. Sci. 42, 1983.
[26] P. Hänggi, *Colored noise in continuous dynamical system*, in Noise in Nonlinear Dynamical Systems 1, F. Moss and P. V. E. McClintock, eds., Cambridge University Press, Cambridge, 1989, pp. 307–347.
[27] P. Hänggi and P. Jung, *Colored noise in dynamical systems*, Adv. Chem. Phys., 89 (1995), pp. 239–326.
[28] R. E. Heath, I. M. Gamba, P. J. Morrison, and C. Michler, *A discontinuous Galerkin method for the Vlasov-Poisson system*, J. Comput. Phys., 231 (2012), pp. 1140–1174.
[29] W. Horsthemke and R. Lefever, *Noise Induced Transitions: Theory and Applications in Physics, Chemistry, and Biology*, Springer Ser. Synergetics 15, Springer, Berlin, 2007.
[30] M. Jardak, C.-H. Su, and G. E. Karniadakis, *Spectral polynomial chaos solutions of the stochastic advection equation*, J. Sci. Comput., 17 (2002), pp. 319–338.
[31] P. Jung and P. Hänggi, *Dynamical systems: A unified colored-noise approximation*, Phys. Rev. A (3), 35 (1987), pp. 4464–4466.
[32] R. P. Kanwal, *Generalized Functions: Theory and Technique*, 2nd ed., Birkhäuser, Boston, 1998.
[33] A. I. Khuri, *Applications of Dirac's delta function in statistics*, Internat. J. Math. Ed. Sci. Tech., 35 (2004), pp. 185–195.
[34] S. B. Kim, *hp-version discontinuous Galerkin methods for hyperbolic conservation laws*, Comput. Methods Appl. Mech. Engrg., 133 (1996), pp. 259–286.
[35] G. Leonenko and T. Phillips, *On the solution of the Fokker-Planck equation using a high-order reduced basis approximation*, Comput. Methods Appl. Mech. Engrg., 199 (2009), pp. 158–168.
[36] J. Li and J.-B. Chen, *Stochastic Dynamics of Structures*, Wiley, Hoboken, NJ, 2009.
[37] W. Y. Liu, W. Q. Zhu, and Z. L. Huang, *Effect of bounded noise on chaotic motion of Duffing oscillator under parametric excitation*, Chaos Solitons Fractals, 12 (2001), pp. 527–537.
[38] T. S. Lundgren, *Distribution functions in the statistical theory of turbulence*, Phys. Fluids, 10 (1967), pp. 969–975.
[39] R. Mankin, T. Laas, A. Sauga, A. Ainsaar, and E. Reiter, *Colored-noise-induced Hopf bifurcations in predator-prey communities*, Phys. Rev. E (3), 74 (2006), 021101.
[40] F. Moss and P. V. E. McClintock, eds., *Noise in Nonlinear Dynamical Systems. Volume* 1: *Theory of Continuous Fokker-Planck Systems*, Cambridge University Press, Cambridge, 1989.
[41] F. Nobile, R. Tempone, and C. G. Webster, *A sparse grid stochastic collocation method for partial differential equations with random input data*, SIAM J. Numer. Anal., 46 (2008), pp. 2309–2345.
[42] A. Nouy, *Proper generalized decompositions and separated representations for the numerical solution of high dimensional stochastic problems*, Arch. Comput. Methods Appl. Mech. Engrg., 17 (2010), pp. 403–434.
[43] A. Nouy and O. P. Le Maître, *Generalized spectral decomposition for stochastic nonlinear problems*, J. Comput. Phys., 228 (2009), pp. 202–235.
[44] E. Novak and K. Ritter, *Simple cubature formulas with high polynomial exactness*, Constr. Approx., 15 (1999), pp. 499–522.
[45] J.-F. Remacle, J. E. Flaherty, and M. S. Shephard, *An adaptive discontinuous Galerkin technique with an orthogonal basis applied to compressible flow problems*, SIAM Rev., 45 (2003), pp. 53–72.
[46] H.-K. Rhee, R. Aris, and N. R. Amundson, *First-Order Partial Differential Equations, Volume* 1: *Theory and Applications of Single Equations*, Dover, Mineola, NY, 2001.
[47] H. Risken, *The Fokker-Planck Equation: Methods of Solution and Applications*, 2nd ed., Math. Sci. Engrg. 60, Springer-Verlag, Berlin, 1989.
[48] P. L. Roe, *Approximate Riemann solvers, parameter vectors and difference schemes*, J. Comput. Phys., 43 (1981), pp. 357–372.
[49] Y. Saad, *Analysis of some Krylov subspace approximations to the matrix exponential operator*, SIAM J. Numer. Anal., 29 (1992), pp. 209–228.
[50] S. Sadooghi-Alvandi, A. Nematollahi, and R. Habibi, *On the distribution of the sum of independent uniform random variables*, Statist. Papers, 50 (2002), pp. 171–175.
[51] T. Sapsis and G. Athanassoulis, *New partial differential equations governing the response-excitation joint probability distributions of nonlinear systems under general stochastic excitation*, Probab. Engrg. Mech., 23 (2008), pp. 289–306.

[52] T. P. Sapsis and P. F. J. Lermusiaux, *Dynamically orthogonal field equations for continuous stochastic dynamical systems*, Phys. D (3), 238 (2009), pp. 2347–2360.
[53] R. L. Stratonovich, *Topics in the Theory of Random Noise: Vols.* 1 *and* 2, Gordon and Breach, New York, 1967.
[54] M. Thalhammer, *High-order exponential operator splitting methods for time-dependent Schrödinger equations*, SIAM J. Numer. Anal., 46 (2008), pp. 2022–2038.
[55] D. Venturi, *On proper orthogonal decomposition of randomly perturbed fields with applications to flow past a cylinder and natural convection over a horizontal plate*, J. Fluid Mech., 559 (2006), pp. 215–254.
[56] D. Venturi, *A fully symmetric nonlinear biorthogonal decomposition theory for random fields*, Phys. D, 240 (2011), pp. 415–425.
[57] D. Venturi, M. Choi, and G. E. Karniadakis, *Supercritical quasi-conduction states in stochastic Rayleigh-Bénard convection*, Internat. J. Heat Mass Transfer, 55 (2012), pp. 3732–3743.
[58] D. Venturi and G. E. Karniadakis, *Differential constraints for the probability density function of stochastic solutions to the wave equation*, Internat. J. Uncertainty Quantification, 2 (2012), pp. 131–150.
[59] D. Venturi and G. E. Karniadakis, *New evolution equations for the joint response-excitation probability density function of stochastic solutions to first-order nonlinear PDEs*, J. Comput. Phys., 231 (2012), pp. 7450–7474.
[60] D. Venturi, T. P. Sapsis, H. Cho, and G. E. Karniadakis, *A computable evolution equation for the probability density function of stochastic dynamical systems*, R. Soc. Lond. Proc. Ser. A Math. Phys. Eng. Sci., 468 (2012), pp. 759–783.
[61] D. Venturi, X. Wan, and G. E. Karniadakis, *Stochastic low-dimensional modelling of a random laminar wake past a circular cylinder*, J. Fluid Mech., 606 (2008), pp. 339–367.
[62] D. Venturi, X. Wan, and G. E. Karniadakis, *Stochastic bifurcation analysis of Rayleigh-Bénard convection*, J. Fluid. Mech., 650 (2010), pp. 391–413.
[63] X. Wan and G. E. Karniadakis, *An adaptive multi-element generalized polynomial chaos method for stochastic differential equations*, J. Comput. Phys., 209 (2005), pp. 617–642.
[64] X. Wan and G. E. Karniadakis, *Multi-element generalized polynomial chaos for arbitrary probability measures*, SIAM J. Sci. Comput., 28 (2006), pp. 901–928.
[65] C.-J. Wang, *Effects of colored noise on stochastic resonance in a tumor cell growth system*, Phys. Scripta., 80 (2009), 065004.
[66] D. Xiu and G. E. Karniadakis, *The Wiener–Askey polynomial chaos for stochastic differential equations*, SIAM J. Sci. Comput., 24 (2002), pp. 619–644.
[67] Y. Xu, R. Gu, H. Zhang, W. Xu, and J. Duan, *Stochastic bifurcations in a bistable Duffing-Van der Pol oscillator with colored noise*, Phys. Rev. E (3), 83 (2011), 056215.
[68] X. Yang, M. Choi, and G. E. Karniadakis, *Adaptive ANOVA decomposition of stochastic incompressible and compressible fluid flows*, J. Comput. Phys., 231 (2012), pp. 1587–1614.
[69] L. Zhang, A. Song, and J. He, *Effect of colored noise on logical stochastic resonance in bistable dynamics*, Phys. Rev. E (3), 82 (2012), 051106.
[70] X. Zhang and C. W. Shu, *On positivity preserving high order discontinuous Galerkin schemes for compressible Euler equations on rectangular meshes*, J. Comput. Phys., 229 (2010), pp. 8918–8934.